Journal of Fluorine Chemistry 131 (2010) 791–799

Contents lists available at ScienceDirect

Journal of Fluorine Chemistry

journal homepage: www.elsevier.com/locate/fluor

Selenium(IV) fluoride and oxofluoride anions

Karl O. Christe [a,*], David A. Dixon [b], Ralf Haiges [a,*], Mathias Hopfinger [a], Virgil E. Jackson [b], Thomas M. Klapötke [c,*], Burkhard Krumm [c], Matthias Scherr [c]

[a] Loker Research Institute and Department of Chemistry, University of Southern California, Los Angeles, CA 90089-1661, USA
[b] Department of Chemistry, University of Alabama, Tuscaloosa, AL 35487-0336, USA
[c] Department of Chemistry, Ludwig-Maximilian University of Munich, Butenandtstr. 5-13(D), D-81377 Munich, Germany

ARTICLE INFO

Article history:
Received 13 March 2010
Received in revised form 15 April 2010
Accepted 20 April 2010
Available online 28 April 2010

Keywords:
Selenium fluorides
Selenium oxofluorides
Multinuclear NMR spectroscopy
X-ray crystallography
Theoretical calculations

Dedicated to Prof. Dr. Henry Selig on the occasion of his ACS Fluorine Award.

ABSTRACT

The $[((C_6H_5)_3P)_2N]^+$, $[(C_6H_5)_4P]^+$ and $[N(CH_3)_4]^+$ salts of SeF_5^-, SeF_6^{2-} and $SeOF_3^-$ and $CsSeO_2F$ were prepared and characterized. Crystal structures were obtained for $[((C_6H_5)_3P)_2N][SeF_5]$ and $[((C_6H_5)_3P)_2N][SeOF_3]$ CH_2Cl_2. In contrast to oxygen-bridged dimeric $TeOF_3^-$, the $SeOF_3^-$ anion in $[((C_6H_5)_3P)_2N][SeOF_3]$ CH_2Cl_2 is monomeric and represents the first experimentally well determined molecular structure of a monomeric trifluoro-chalcogenite anion. Similarly, $[((C_6H_5)_3P)_2N][SeF_5]$ represents the first example of a structure containing a well-isolated undistorted SeF_5^- anion. The NMR and the vibrational spectra and their assignments were re-examined and corrected by comparison with high-level theoretical calculations. Whereas the previously published normal coordinate analysis of SeF_5^- is correct, that for $SeOF_3^-$ needs major revision.

1. Introduction

The properties of the binary selenium(IV)–fluorine compounds SeF_4 [1–5], SeF_5^- [6,7], and SeF_6^{2-} [8,9] have been studied for a number of years. The oxygen containing selenium(IV) fluorides $SeOF_2$ [10–14], SeO_2F^- [15–19], and $SeOF_3^-$ [20–22] have also been studied. A calculated structure of SOF_3^- [23] and the molecular structure of the $TeOF_3^-$ dimer, $[Te_2O_6F_2]^{2-}$, [24,25] have been reported, but the selenium analogue $SeOF_3^-$ had only been characterized by vibrational spectroscopy. Furthermore, for SeF_5^-, , only the crystal structure of a tetrameric anion is known [6], which was strongly distorted from the ideal C_{4v} geometry predicted [26–28] for the free anion. In this paper, we present a reinvestigation of the above selenium(IV) compounds and also the crystal structures of the monomeric SeF_5^- anion and the trifluoroselenite anion, $SeOF_3^-$.

2. Results and discussion

2.1. Synthesis

The selenium fluorides $[PNP][SeF_5]$ and $[PNP]_2[SeF_6]$, ($PNP^+ = [((C_6H_5)_3P)_2N]^+$), were synthesized (at LMU) by reaction of selenium tetrafluoride with one and two equivalents of silver fluoride, respectively, to form the corresponding silver salts. The subsequent reactions with equimolar amounts of [PNP]Cl resulted in the formation of insoluble AgCl and the corresponding PNP-salts. The single crystals of $[PNP][SeOF_3]\cdot CH_2Cl_2$ were obtained by the hydrolysis of $[PNP][SeF_5]$ in CH_2Cl_2 solution with small amounts of adventitious water.

The selenium fluorides $A[SeF_5]$, $A_2[SeF_6]$ and $A[SeOF_3]$ (A = tetramethyl ammonium, TMA^+, tetraphenyl phosphonium, TPP^+, and PNP^+) were prepared (at USC) by reaction of stoichiometric amounts of SeF_4 and $SeOF_2$, respectively, with the corresponding poly-bifluorides $A[HF_2\cdot x\,HF]$ in acetonitrile solution. The SeF_4 was prepared in high yield and purity by the reaction of SeO_2 with ClF_3 in HF solution at room temperature, and the $SeOF_2$ by conproportionation of SeO_2 and SeF_4 at room temperature. The $Cs[SeO_2F]$ salt was prepared from CsF and H_2SeO_3 in aqueous solution by a literature method [16].

2.2. NMR spectra

All compounds were characterized by ^{19}F and ^{77}Se NMR spectroscopy (Table 1). At room temperature, the ^{19}F and ^{77}Se NMR resonances were generally broad and it was not possible to observe any F–F couplings. For SeF_5^- in either DMSO or CH_3CN solution, two ^{19}F resonances were observed at about 18 and 57 ppm with an area ratio of 4:1. These resonances can be attributed to the four

* Corresponding authors.
E-mail addresses: kchriste@usc.edu (K.O. Christe), haiges@usc.edu (R. Haiges), tmk@cup.uni-muenchen.de (T.M. Klapötke).

0022-1139/$ – see front matter © 2010 Elsevier B.V. All rights reserved.
doi:10.1016/j.jfluchem.2010.04.009

Table 1
Experimentally observed and computed ^{19}F and ^{77}Se NMR chemical shifts.

Molecule	δ (^{19}F)/ppm[a]		δ (^{77}Se)/ppm[b]	
	Expt.[c]	Calc.	Expt.[c]	Calc.[d,e,f]
SeF_4 (CH_3F, −140 °C[b], −135 °C[c])	37.7, t[g] 12.1, t[g]	ax 86[d], 83[e], 76[f], 55[h] eq 56[d], 49[e], 49[f], 16[h]	1083[i]	1042[d], 1159[e], 1162[f], 1100[h], 1153[j]
SeF_4 (CH_3F, 20 °C)[b]	28.7			
SeF_4 (CD_2Cl_2, 0 °C)	32.1		1120	
SeF_4 (CH_3CN, 25 °C)	20.2		1093	
SeF_4 (neat, 25 °C)	18.4, 24.9[k], 27.5[l]		1114, 1092[m]	
[TPP][SeF_5] (DMSO, 25 °C)	57.7 br (1 F) 19.6 br (4 F)	eq 79[d], 56[e], 67[f] ax 29[d], 10[e], 20[f]	970, d[k]	880[d], 1001[e], 1053[f]
[TPP][SeF_5] (CH_3CN, 25 °C)	56.2 br (1 F) 17.2 br (4 F)		962	
[TMA][SeF_5] (CH_3CN)	14.4[n]			
[TMA]$_2$[SeF_6] (CH_3CN, 25 °C)	43.9 br	0[d], −32[e], −12[f]	1255	945[d], 1088[e], 1211[f]
[PNP]$_2$[SeF_6] (CD_2Cl_2, 0 °C)	41.5 br		1253	
$SeOF_2$ (CH_3CN, 25 °C)	34.6	69[d], 70[e], 59[f]	1398 t[o]	1267[d], 1370[e], 1303[f], 1402[l]
$SeOF_2$ (CD_2Cl_2, 0 °C)	42.8		1397 t[p]	
$SeOF_2$ (neat)	37.0 br, 38.6[q]		1392, 1378[i,m,r]	
[TMA][$SeOF_3$] (CH_3CN, 25 °C)	19.0 br	ax 44[d], 21[e], 31[f] eq 43[d], 28[e], 37[f]	1358	1129[d], 1261[e], 1230[f]
[TPP][$SeOF_3$] (CH_3CN, 25 °C)	16.1		1385	
$CsSeO_2F$ (D_2O, 25 °C)	Not observed	45[d], 24[e], 40[f]	1314	1376[d], 1511[e], 1383[f]

[a] F chemical shifts relative to $CFCl_3$. Absolute F chemical shift = 156.1 ppm at the GIAO B3LYP/AhlrichsVTZP level; absolute F chemical shift = 135.3 ppm at the GIAO BLYP/TZ2P level with the ADF code.
[b] Se chemical shifts relative to $Se(CH_3)_2$. Absolute Se chemical shift = 1698.8 ppm at the GIAO B3LYP/AhlrichsVTZP level; absolute Se chemical shift = 1616.2 ppm at the GIAO BLYP/TZ2P level with the ADF code.
[c] Data from this study, unless noted otherwise.
[d] Data from this study, MPW1PW91/aug-cc-pVDZ.
[e] Data from this study, GIAO B3LYP/AhlrichsVTZP.
[f] Data from this study, BLYP-ZORA/TZ2P.
[g] Data from Ref. [3].
[h] Data from [46] using GIAO-MP2/6-311 + G(3df,3pd)//MP2/6-311 + G(3df,3pd).
[i] Data from Ref. [5].
[j] Data from [47] using PBE0/TZVP(P)//PBE0/TZVP.
[k] Data from C. Lau, J. Passmore, J. Fluorine Chem. 6 (1975) 77–81.
[l] Data from G.A. Olah, M. Nojima, I. Kerekes, J. Am. Chem. Soc. 46 (1974) 925–927.
[m] Data from R. Birchall, J. Gillespie, S.L. Vekris, Can. J. Chem. 43 (1965) 1672–1679.
[n] Data from Ref. [6].
[o] J(SeF) 786 Hz.
[p] J(SeF) 854 Hz.
[q] Data from [k].
[r] J(SeF) 837 Hz from [k].

equatorial and one axial fluorine atoms of the anion possessing a C_{4v} structure, which was also found in the crystal structure (see below). ^{77}Se satellites could only be observed for the axial fluorine signal at 57.7 ppm in DMSO ($^1J(SeF_{ax})$ = 1170 Hz). This assignment is further substantiated by the observed broad doublet at 970 ppm in the ^{77}Se NMR spectrum of this sample, which exhibits the same $^1J(SeF_{ax})$ coupling constant. The failure to observe the coupling to the four equatorial fluorines is attributed to the broadness of the signals and the small value expected for this coupling. In the structurally related C_{4v} molecule, ClF_5, $^1J^{35}Cl^{19}F_{ax}$ was found to be 192 Hz, whereas $^1J^{35}Cl^{19}F_{eq}$ was ≤20 Hz [29]. It is interesting to note, that the ^{77}Se NMR spectrum of the $[SeF_5]^-$ anion in CH_3CN solution showed only a broad singlet at 962 ppm, indicating a more fluxional structure than in DMSO solution. The only previously reported value for the NMR spectra of SeF_5^- was a broad signal at 14.4 ppm in the ^{19}F spectrum, recorded for $[TMA]^+[SeF_5]^-$ in CH_3CN at an unspecified temperature [6]. It appears that this signal may have been due to the four equatorial fluorines with the axial fluorine signal not having been observed or reported.

For the $[SeF_6]^{2-}$ anion, our values are also somewhat at odds with the previous literature report [8] which listed no ^{77}Se signal and a single resonance without ^{77}Se satellites at 13.4 ppm for the ^{19}F NMR spectrum of the $[PIP^+]_2[SeF_6]^{2-}$ salt (PIP^+ = 1,13,3,5,5-hexamethylpiperidinium) in CH_3CN solution at an unspecified temperature. This ^{19}F signal was shifted to higher values upon addition of SeF_5^- and to lower values upon addition of F^-, which was interpreted in terms of a rapid intermolecular fluorine exchange between SeF_5^-, SeF_6^{2-} and F^-; however, it should be noted that this signal is very close to that reported by these authors [8] for SeF_5^- and, therefore, might have been due to the latter. In our current study, broad resonances were observed at about 43 ppm in the ^{19}F and at about 1254 ppm in the ^{77}Se spectra of SeF_6^{2-} in either CH_3CN or CH_2Cl_2 solution. Whereas the ^{19}F resonances of SeF_6^{2-} (43 ppm) and exchange-averaged equatorial/axial SeF_5^- (26 ppm) are similar and, therefore, do not allow a clear distinction between SeF_5^- and SeF_6^{2-}, our ^{77}Se resonances of SeF_5^- (970 ppm) and SeF_6^{2-} (1254 ppm) differ by a very large amount and imply that the spectra observed by us for SeF_6^{2-} are not largely due to a mixture of rapidly exchanging SeF_5^- and F^-. A substantial difference in the ^{77}Se resonances of SeF_5^- (970 ppm) and SeF_6^{2-} is consistent with the calculations discussed below.

In Table 1, the experimentally observed shifts are also compared to values calculated at the density functional theory level using GIAO [30] to deal with the gauge problem with different exchange-correlation functionals and basis sets: MPW1PW91/aug-cc-pVDZ [31–34], B3LYP/AhlrichsVTZP [35–37], BLYP/TZ2P

[38,39], and at the ZORA-BLYP/TZ2P level to include the effects of relativity [40–45]. We also compare to previous calculated results at the MP2/6-311 + G(3df,3pd)//MP2/6-311 + G(3df,3pd) [46] and PBE0/TZVP(P)//–PBE0/TZVP [47] levels of theory. In general, the calculated ^{19}F shifts reflect the observed trends reasonably well. The best results for SeF_4 are those at the MP2 level [46]. The effects of relativity at the ZORA level with the BLYP functional are small for the ^{19}F chemical shifts. In general the DFT values are up to 30–50 ppm too large as compared to experiment.

The calculated ^{77}Se chemical shifts are in qualitative agreement with experiment. For SeF_4 and SeF_5^-, the calculated chemical shifts bracket the experimental values. As noted previously [47,48] calculations of ^{77}Se shifts are quite sensitive to small changes in the geometry, solvent used, temperature and computational methods and, therefore, show larger variations than the calculated ^{19}F shifts. The effect of the relativistic correction for the Se chemical shifts can be to either increase or decrease the chemical shift. For $SeOF_2^-$, the calculated chemical shifts are greater than experiment, whereas for SeF_6^{2-}, $SeOF_2$, and $SeOF_3^-$ the calculated values are smaller than experiment. The observed experimental trend that the chemical shift of SeF_5^- is less than that of SeF_6^{2-} is confirmed by the calculations.

For the ^{19}F chemical shifts, the only exception for the calculated chemical shifts being larger than experiment is for $SeF_6^{2-}$where the trend is in the opposite direction and the calculated ^{19}F chemical shifts are more negative than experiment. This is no surprise because the free valence electron pair of Se is partially sterically active [8,49] requiring very high-level computations for reliable results [50–53]. The structures of the isoelectronic molecules KrF_6 and BrF_6^- are octahedral but the structures of XeF_6 and IF_6^- are C_{3v} with the octahedral structure slightly higher in energy. We attempted to reproduce the previous calculations [49] for SeF_6^{2-} at the B3LYP/6-311 + G(2df) level but were unable to obtain a C_{3v} structure lower than the O_h structure. We note that the previous calculations predicted the C_{3v} structure to be only 0.4 kcal/mol below the O_h structure. We also note that using the same approach the previous authors [49] predicted that KrF_6, BrF_6^-, and AsF_6^{3-} are all octahedral even though the lone pair would be expected to be larger in the latter than in SeF_6^{2-}. Our B3LYP/aVTZ-PP calculations as well as previous [27,54] calculations resulted in a sterically inactive valence electron pair on Se and an O_h geometry. In addition, starting from the C_{3v} structure, we optimized the geometry at the CCSD(T)/aug-cc-pVTZ level and found an O_h structure. In order to further study this issue, we used the same approach as we did for XeF_6 as well as IF_6^- and calculated the energy difference between the O_h and C_{3v} structures for SeF_6^{2-} at the CCSD(T) level as a function of the basis set. We were able to optimize the O_h structure at the CCSD(T) level but had to use estimated structures for the C_{3v} conformer. We used the Hartree–Fock structure, the reported DFT optimized structure and the experimental crystal structure. The energy differences are strongly basis set dependent as shown in Table 2.

2.3. Crystal structures

Colorless crystals of $[PNP][SeOF_3]\cdot CH_2Cl_2$ were obtained by storing a concentrated solution of $[PNP][SeF_5]$ in CH_2Cl_2 at −32 °C over night at LMU. When taken out of the solution, the crystals rapidly decomposed upon contact with air at room temperature. Therefore, a crystal was mounted on the goniometer head under an inert atmosphere at 253 K and immediately transferred into the cold nitrogen stream of the diffractometer. The resulting structure was that of the PNP-salt of the trifluoroselenite anion, $SeOF_3^-$, containing one molecule of disordered dichloromethane as a solvate, $[PNP][SeOF_3]\cdot CH_2Cl_2$. The formation of this anion can be explained by the reaction of $[PNP][SeF_5]$ with traces of adventitious water.

$[PNP][SeOF_3]\cdot CH_2Cl_2$ crystallizes in the triclinic crystal system, space group $P\bar{1}$ with $Z = 2$ (Table 3). The $SeOF_3^-$ anion (Fig. 1) adopts a pseudo-trigonal bipyramidal structure with two fluorine atoms in the axial positions and the three equatorial positions being occupied by an oxygen, a fluorine and a sterically active free

Table 2
O_h–C_{3v} energy differences for SeF_6^{2-} at the CCSD(T) level in kcal/mol.

Method	aug-cc-pVDZ	aug-cc-pVTZ	aug-cc-pVQZ
DFT[a]	13.1	12.2	12.4
Exp[b]	14.8	10.6	10.1
HF[c]	23.0	11.1	9.6

[a] Geometry parameters for the C_{3v} structure: r(Se–F) = 1.907 and 2.051 Å.
[b] r(Se–F) = 1.840 and 2.03 Å.
[c] r(Se–F) = 1.719 and 2.167 Å.

Table 3
Summary of crystal data and refinement results.

Property	$[PNP][SeOF_3]$	$[PNP][SeF_5]$
Empirical formula	$C_{36}H_{30}F_3NOP_2Se$	$C_{36}H_{30}F_5NP_2Se$
Formula mass	690.53	712.51
Temperature [K]	100	298
Crystal size [mm]	0.42 × 0.28 × 0.27	0.24 × 0.16 × 0.11
Space group	$P\bar{1}$	$C2/c$
a [Å]	11.7382(11)	16.1712(12)
b [Å]	11.8451(10)	13.7199(10)
c [Å]	14.1545(14)	16.0646(12)
α [°]	66.790(9)	90
β [°]	70.321(9)	112.961 (1)
γ [°]	71.023(8)	90
V [Å^3]	1660.5(3)	3281.8(4)
Z	2	4
ρ_{calc} [g cm^{-3}]	1.3811	1.442
μ [mm^{-1}]	1.273	1.297
Reflections collected	11647	9937
Reflections unique	9652 (R_{int} = 0.0187)	3687 [R_{int} = 0.0475]
$R1$, $wR2$ (2σ data)	0.0429, 0.0855	0.0395, 0.0922
$R1$, $wR2$ (all data)	0.0527, 0.0963	0.0612, 0.0961
GOOF on F^2	1.138	1.009

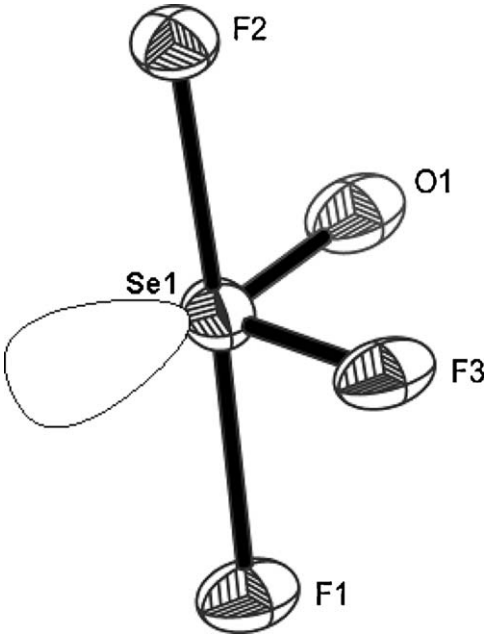

Fig. 1. Molecular structure of the $SeOF_3^-$ anion in $[PNP][SeOF_3]$. Thermal ellipsoids are shown at the 50% probability level. Selected bond lengths [Å] and angles [°]: Se1–F1 1.9020(10), Se1–F2 1.906(3), Se1–O1 1.609(3), Se1–F3 1.7668(10), F2–Se1–F1 174.79(10), F1–Se1–F3 90.70(11), F2–Se1–F3 87.52(11), F1–Se1–O1 91.80(12), F2–Se1–O1 93.39(12), F3–Se1–O1 104.32(17).

Table 4
Comparison of the experimental and calculated (CCSD(T) and DFT) structures of $SeOF_3^-$ with those of isoelectronic $BrOF_3$[55] and of closely related $ClOF_3$[56].[a]

Parameter	$SeOF_3^-$	CCSD(T)/aug-cc-pVQZ	B3LYP/aug-cc-pVQZ	$BrOF_3$	$ClOF_3$
$X–F_{ax}$	1.906(3) 1.902(1)	1.901	1.923	182.0(3) 183.9(4)	1.713(3)
$X–F_{eq}$	1.767(1)	1.763	1.781	1.725(3)	1.603(4)
X–O	1.609(3)	1.599	1.595	1.569(4)	1.405(3)
$F_{ax}–X–F_{ax}$	174.8(1)	167.9	166.3	169.8(2)	170.5(41)
$F_{eq}–X–O$	104.3(2)	104.1	104.2	103.3(2)	108.9(9)
$F_{eq}–X–F_{ax}$	87.5(1) 90.7(1)	86.8	86.1	86.3(2)	87.9(12)
$O–X–F_{ax}$	91.8(1) 93.4(1)	95.8	96.4	94.3(2)	94.7(20) 94.7(20)

[a] Bond lengths in Å, angles in degree.

valence electron pair. This structure is analogous to those previously found for isoelectronic $BrOF_3$ [55] and the related $ClOF_3$ molecule [56] (Table 4). The structure of $SeOF_3^-$ is in excellent agreement with our theoretical calculations (Table 4), showing that the oxygen and the equatorial fluorine are not suffering from disorder. Although theoretical calculations were carried out at different levels of theory and with different basis sets, only those obtained at the highest levels (CCSD(T)) with the best basis sets are given in Table 4. As expected, the results from the coupled cluster calculations are superior to those using density functional theory.

Consistent with the experimental structures of $BrOF_3$ [55] and $ClOF_3$ [56] and the calculated structure of the analogous sulfur compound, SOF_3^- [23], the axial Se–F bond lengths in $SeOF_3^-$ are significantly longer than the equatorial one and, as expected, longer than those in SOF_3^-, $ClOF_3$ and $BrOF_3$. The bond lengthening in $SeOF_3^-$, when compared to the neutral $BrOF_3$ molecule, is due to the formal negative charge in $SeOF_3^-$ which increases the ionicity of the bonds and makes them longer. The fact that the bond length of the axial Se–F bonds is much larger than that of the equatorial one suggests that the negative charges in $SeOF_3^-$ are larger on the two axial fluorine atoms (Mulliken charge $q = -0.70$e (B3LYP/aug-cc-pVTZ)) than on the equatorial fluorine atom ($q = -0.59$e). Therefore, the bonding in $SeOF_3^-$ is best described by a model assuming a semi-ionic *3c–4e* bond [57,58] for the two axial fluorine ligands and predominantly covalent bonding for the equatorial fluorine and oxygen ligands, as discussed below in more detail for SeF_5^-. The Se–O distance is significantly shorter than the equatorial Se–F distance implying that the Se–O bond has high double bond character the nature of which has recently been analyzed [59] using the Bader's AIM method [60]. By analogy with $BrOF_3$ and $ClOF_3$, the axial fluorine atoms are bent away from the Se=O double bond into the sector between the Se–F single bond and the free lone electron pair of Se. This demonstrates that in the axial direction the steric repulsion from the Se=O double bond is larger than the repulsion from either the lone pair on Se or the Se–F single bond. The angles in the equatorial plane [56], however, show that in the equatorial direction the repulsion by the lone pair is largest, followed by the Se=O double bond, with the Se–F single bond being smallest consistent with VSEPR arguments. These directional repulsion effects by lone valence electron pairs and π bonds in trigonal bipyramidal molecules have been discussed by us in detail previously [61]. A discussion of trends within the SOF_3^-, $SeOF_3^-$, and $TeOF_3^-$ series is not warranted at this point because for SOF_3^- only a low-level calculated structure is available, and for $TeOF_3^-$ the experimental structure contains oxygen-bridged dimeric anions [24] which are also present in the complex salt $[C_5H_6N]_2[TeF_5][Te_2O_2F_6]_{0.5}$ [25]. Therefore, the crystal structure of $SeOF_3^-$ represents the first experimentally well-determined molecular structure of a monomeric trifluoro-chalcogenite anion.

Slightly pink single crystals of $[PNP][SeF_5]$ were grown from CH_3CN solution by slow evacuation of the solvent in *vacuo* at −20 °C at USC. The compound crystallizes in the monoclinic space group *C2/c* with $Z = 4$ (Table 3). In contrast to the previously reported [6] crystal structure of $[N(CH_3)_4][SeF_5]$, which contains tetrameric $[SeF_5^-]_4$ units in which the individual anions are strongly distorted from the ideal C_{4v} symmetry, $[PNP][SeF_5]$ contains well-isolated SeF_5^- anions with almost perfect square pyramidal symmetry (Fig. 2). The axial Se–F bond length of 1.68 Å is significantly shorter than the equatorial ones of 1.81 Å, in excellent accord with Christe's Rule III for hypervalent species containing a sterically active free valence electron pair [62]. This rule states that "the free valence electron pairs on the central atoms seek high *s*-character, i.e., sp^n hybridization. If the number of ligands (including the free electron pairs) is larger than four, then so many F ligands form linear semi-ionic 3 center −4 electron (*3c–4e*) bonds [57,58] as are required to allow the free electron pairs to form an sp^n hybrid with the remaining F ligands. These semi-ionic *3c–4e* bonds are significantly weaker and longer than the mainly covalent sp^n hybrid bonds." The increased polarity of the four equatorial Se–F bonds in SeF_5^- is also reflected by the Mulliken charges of −0.60 and −0.81 calculated by us at the B3LYP/aug-cc-pVTZ level for the axial and the four equatorial bonds, respectively. Because the free valence electron pair of selenium is more diffuse and space-demanding than the bonding electron pairs, the $F_{ax}–Se–F_{eq}$ angles are slightly compressed from the ideal value of 90–84°. The $[SeF_5]^-$ anions are located in channels, formed by the cations, with the axial F ligands pointing up and down in an alternating pattern. They are very well separated because of the rather large

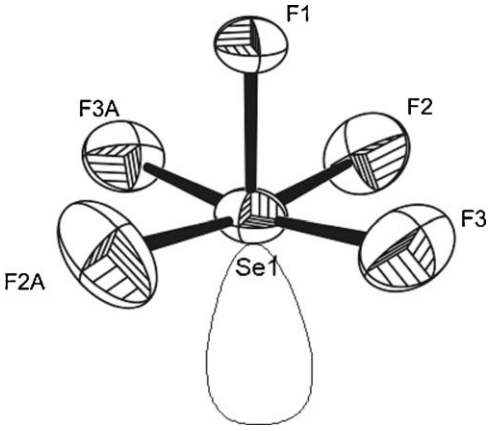

Fig. 2. Molecular structure of the SeF_5^- anion in $[PNP][SeF_5]$. Thermal ellipsoids are shown at the 50% probability level. Selected bond lengths [Å] and angles [°]: Se–F1 1.681(2), Se–F2 1.809(2), Se–F3 1.812(2), F1–Se–F2 84.46(8), F1–Se–F3 84.13(7), F2–Se–F3 90.31(11), F2–Se–F2A 168.92(16), F3–Se–F3A 168.25(13).

Table 5
Computational and experimental geometries for SeF_5^- (bond lengths in Å, angles in degree).

Parameter	MPW1PW91/aug-cc-PVDZ	CCSD(T)/aug-cc-pVQZ	Exptl. [PNP][SeF_5]	Exptl.[a] [TMA][SeF_5]
Point group	C_{4v}	C_{4v}		
Se–F_{ax}	1.752	1.715	1.681(2)	1.707(3) 1.717(3)
Se–F_{eq}	1.863	1.836	1.809(2) 1.812(2)	1.827(3) 1.869(3)
F_{ax}–Se–F_{eq2}	84.7	84.2	84.46(8)	83.1(1)
F_{ax}–Se–F_{eq3}	84.7	84.2	84.13(7)	84.3(1)
F_{eq2}–Se–F_{eq2A}	169.4	168.4	168.92(16)	166.2(2)
F_{eq3}–Se–F_{eq3A}	169.4	168.4	168.25(13)	168.6(2)

[a] Data from Reference [6].

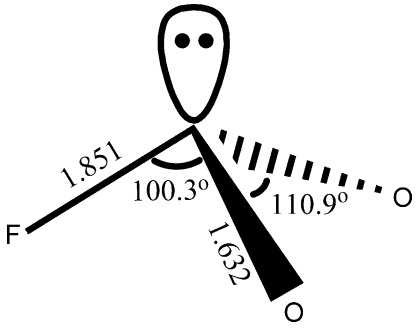

Fig. 3. Structure of the SeO_2F^- anion, calculated at the CCSD(T)/aug-cc-pVQZ level of theory. Selected bond lengths [Å] and angles [°]: Se–F 1.851, Se–O 1.632, F–Se–O 100.3, O–Se–O 110.9.

$[PNP]^+$ counter-ions, and the closest Se–F distances between neighboring anions are 6.4 Å. Table 5 shows a comparison of the experimental structure [6] of tetrameric SeF_5^- in [TMA][SeF_5] and our structure of monomeric SeF_5^- in [PNP][SeF_5] with values calculated for the free gaseous anion at different levels of theory. The agreement between the two experimental structures is quite good in spite of the association in the TMA salt, and the fit with the coupled cluster CCSD(T) calculations is excellent.

Since we could not obtain a well ordered crystal structure for the SeO_2F^- anion, we have calculated its structure at the CCSD(T)/aug-cc-pVQZ level of theory (Fig. 3). In this anion, Se has only a coordination number of 4, so it is not hypervalent and no semi-ionic *3c–4e* bonding contributions need to be invoked. Compared to the calculated structure for neutral SeO_2 ($r_{Se=O}$ = 1.611 Å), the Se=O bond distance (1.632 Å) in SeO_2F^- has increased only slightly, but the Se–F bond length (1.851 Å) is unusually long. Therefore, the Se–F bond is highly ionic and carries most of the negative charge. Inspection of the CCSD(T)/aug-cc-pVQZ values for the Se–F bonds in the Se(+IV) anion series, SeO_2F^- (1.851 Å), $SeOF_3^-$ (unique Se–F = 1.763 Å), SeF_5^- (unique Se–F = 1.715 Å), shows a pronounced shortening from SeO_2F^- to SeF_5^-. This is due to the fact that the electron withdrawing effect of a doubly bonded oxygen is substantially lower than that of two fluorine ligands, thereby causing the unique Se–F bond in SeF_5^- to be the least polar and hence the shortest one.

2.4. Vibrational spectra

The previously reported [7] vibrational spectra of $CsSeF_5$ and their assignments were examined for their correctness by comparison with those calculated at the MPW1PW91/aug-cc-PVDZ, B3LYP/aug-cc-PVTZ and CCSD(T)/aug-cc-PVDZ levels (Table 6). Whereas the observed stretching mode frequencies are slightly lower than the calculated ones, the observed deformation mode frequencies are higher than the calculated ones. The calculated stretches are higher than experiment due to the lack of anharmonic corrections and the bends are predicted to be too low as is typically found for these types of compounds. The biggest differences are ~40 cm^{-1} between theory and experiment for the ν_7 stretch and the ν_5 and ν_8 bends. The excellent agreement between theory and experiment confirms our assignments.

Vibrational data of alkali trifluoroselenites have been known for many years [20–22], and a complete normal coordinate analysis had been carried out previously [20]. However, a comparison with our calculated spectra (Table 7) reveals that in the previous assignments, the antisymmetric axial SeF_2 stretching frequency had been misassigned to a band having [26,27] too high a frequency, resulting in a value for the axial stretching force constant which is much too high. In addition, ν_4, ν_5, ν_8, and ν_9 were assigned incorrectly, and some of the mode descriptions were misleading. By analogy to the closely related pseudo-trigonal bipyramidal SF_4 molecule [63], the axial and equatorial scissoring

Table 6
Observed and calculated vibrational frequencies (cm^{-1}) of SeF_5^- and their assignments in point group C_{4v}.

Assignment IR, RA activ	Approx mode descript	$CsSeF_5$ [7] obsd freq, rel intens		Calcd freq, (IR) [RA] intens[a] MPW1PW91/aug-cc-pVDZ	Calcd freq, (IR) [RA] intens[a] B3LYP/aug-cc-pVTZ	Calcd freq, (IR) intens CCSD(T)/aug-cc-pVDZ[b]
		RA	IR			
A_1 (RA, IR) ν_1	$\nu_{SeF\ axial}$	666 [10]	665 vs	674 (84) [13]	660 (83) [13]	674 (84)
ν_2	$\nu_{sym\ SeF_4\ in\ phase}$	515 [7.5]	520 sh	524 (2.6) [14]	504 (2.5) [14]	527 (0.01)
ν_3	$\delta_{umbrella}$	332 [3.2]	335 s	311 (31) [2.3]	289 (31) [3.1]	305 (48)
B_1 (RA, –) ν_4	$\nu_{sym\ SeF_4\ out\ of\ phase}$	460 [7.0]	–	469 (0) [14]	443 (0) [13]	475(0)
ν_5	$\delta_{asym\ SeF_4\ out\ of\ plane}$	236 [0.6]	–	183 (0) [0.1]	181 (0) [0.2]	191 (0)
B_2 (RA, –) ν_6	$\delta_{sym\ SeF_4\ in\ plane}$	282 [2.6]	–	259 (0) [2.1]	258 (0) [2.1]	265 (0)
E (RA, IR) ν_7	$\nu_{asym\ SeF_4}$	480 sh	475 vs, br	527 (881) [1.3]	492 (874) [1.3]	526 (393)
ν_8	$\delta_{F'SeF_4}$	399 [1.9]	398 mw	348 (0.2) [1.6]	350 (0.4) [1.4]	359 (4.9)
ν_9	$\delta_{asym\ SeF_4\ in\ plane}$	202 [0.7]	n.o.	188 (0.3) [0.4]	185 (1.4) [0.3]	194 (0.1)

[a] IR intensities in km/mol, RA intensities in $Å^4\,amu^{-1}$.
[b] IR intensities at the CCSD(T)/cc-pVDZ level.

Table 7
Observed and calculated vibrational frequencies (cm^{-1}) of $SeOF_3^-$ and their assignments in point group C_s.

Assignment	Approx mode descript	$CsSeOF_3$ [20] obsd RA freq, rel intens	Calc freq, (IR) [RA] intens[a] MPW1PW91/ aug-cc-pVDZ	Calc freq, (IR) [RA] intens[a] B3LYP/aug-cc-pVTZ	Calc freq, (IR) [RA] intens[a] MP2/aug-cc-pVDZ	Calc freq CCSD(T)/ aug-cc-pVDZ
A′ ν_1	ν_{SeO}	958 [10]	965 (119) [26]	971 (119) [28]	1006 (138) [27]	934
ν_2	$\nu_{SeF_{eq}}$	560 [10]	584 (146) [9.0]	564 (145) [8.6]	570 (159) [13]	581
ν_3	$\nu_{sym\ SeF_{2\,ax}}$	420 [8,br]	440 (5.9) [12]	414 (6.2) [12]	435 (5.4) [16]	440
ν_4	$\delta_{scissOSeF_{eq}} + \delta_{sym\,SeF_{2ax(umbrella)}}$	350 [2]	326 (28) [2.9]	326 (26) [3.1]	330 (29.7) [3.8]	324
ν_5	$\delta_{sym\ SeF_{2\,ax\ out\ of\ F-SeF\ plane}}$	230 [0+]	198 (28) [3]	187 (11) [0.2]	195 (9.4) [0.2]	189
ν_6	$\delta_{sym\ SeF_{2\,ax}} - \delta_{scissOSeF_{eq(Berry\ \ mechanism)}}$	197 [1]	191 (11) [0.2]	162 (6.2) [0.3]	166 (5.2) [0.8]	162
A″ ν_7	$\nu_{asym\ SeF_{2\,ax}}$	420, br	465 (457) [0.3]	431 (436) [0.3]	460 (487) [0.5]	455
ν_8	$\delta_{wagOSeF_{eq}}$	375 [1]	338 (3.5) [2.0]	331 (21) [2.0]	343 (2.8) [2.4]	334
ν_9	$\pi_{OSeF_{eq\,out\ of\ plane}}$	303 [2]	277 (0.2) [1.4]	273 (0.9) [1.4]	282 (0.4) [1.4]	271

[a] IR intensities in km/mol, RA intensities in $Å^4\,amu^{-1}$.

Table 8
Observed and calculated vibrational frequencies (cm^{-1}) of SeO_2F^- and their assignments in point group C_s.

Assignment	Approx mode descript	$CsSeO_2F$[a] obsd RA freq, rel intens	Et_4NSeO_2F[b] obsd (IR) [RA]	Calcd freq, (IR) [RA] intens[c] B3LYP/aug-cc-pVTZ	Calcd freq, CCSD(T)/ aug-cc-pVDZ
A′ ν_1	$\nu_{sym\ SeO_2}$	879 [10]	910 [10]	896 (65) [37]	856
ν_2	ν_{SeF}	429 [2.0]	452 [1]	443 (182) [5.0]	464
ν_3	$\nu_{sciss\ SeO_2}$	402 [2.0]	389 [2]	379 (38) [3.0]	366
ν_4	$\nu_{sym\ FSeO_2}$	320 [1.8]	297 [1]	273 (3.5) [3.6]	270
A″ ν_5	$\nu_{asym\ SeO_2}$	857 [4.4]	864 [1]	900 (267) [16]	869
ν_6	$\delta_{asym\ FSeO_2}$	281 [2.1]	266 [1]	243 (5.5) [2.9]	240

[a] Data from this work.
[b] data from Ref. [16].
[c] IR intensities in km/mol, RA intensities in $Å^4\,amu^{-1}$.

modes are strongly coupled, resulting in a symmetric (ν_4) and antisymmetric (ν_6) combination of the corresponding symmetry coordinates. Therefore, (ν_4) is best described as an umbrella type deformation, while (ν_6) corresponds to the mode which becomes the reaction coordinate for the axial–equatorial fluorine ligand exchange by the Berry mechanism [64]. Again, excellent agreement is found between theory and experiment with the largest difference being $\sim$40 cm^{-1} for the ν_5 and ν_8 bending modes.

The vibrational spectra of the SeO_2F^- anion have previously been reported and analyzed in detail [16]. Since its four lower frequency modes have relatively similar frequencies and intensities, we have calculated its vibrational spectra at the CCSD(T)/aug-cc-pVDZ and B3LYP/aug-cc-pVTZ levels of theory (Table 8) to verify the previously proposed assignments [16]. It was found that our current Raman spectrum for $CsSeO_2F$ was in good agreement with that previously reported and that the previously proposed assignments are also correct. The largest deviations between the calculated and observed frequencies are attributed in part to anion association and solid state effects, because the deviations become smaller with increasing cation size and for solutions of the salts in either CH_3CN or $(CH_3)_2SO$ [16]. We note that the SeO_2 stretching frequencies are calculated to be closer to each other than was experimentally observed and that their order should be reversed with the SeO_2 antisymmetric stretching frequency being higher than the symmetric one.

2.5. Calculated heats of formation

Our composite approach [65] to the prediction of the thermodynamic properties of molecules is based on CCSD(T) calculations extrapolated to the complete basis set limit plus the inclusion of additional corrections. This approach was used to calculate the heats of formation of SeF_5^-, SeO_2F^-, and $SeOF_3^-$ as well as those of SeF_4, SeO_2, and $SeOF_2$ as given in Table 9. These values can be used to predict the fluoride affinities (negative of the binding energy of F^- to A to form AF^-) of the three neutral compounds and they are 75.8, 68.1, and 64.1 kcal/mol for SeF_4, SeO_2, and $SeOF_2$, respectively. The fluoride affinities provide an estimate of the Lewis acidity of a compound [66] and show that these selenium compounds are moderate Lewis acids.

3. Experimental

3.1. General procedures

At LMU, all manipulation of air- and moisture-sensitive materials were performed under an inert atmosphere of dry argon using flame-dried glass vessels or oven-dried plastic equipment and Schlenk techniques [67]. The selenium fluorides were handled in PFA-vessels (perfluoroalkoxy-copolymer) due to the extreme sensitivity towards glass. For all NMR measurements, 4 mm PFA-tubes were used, which were placed into standard 5 mm NMR glass tubes. Selenium tetrafluoride (Galaxy Chemicals), silver fluoride (ABCR) and bis(triphenylphosphoranylidene)ammonium chloride ([PNP]Cl, Aldrich) were used as received. The salts $[PNP][SeF_5]$ and $[PNP]_2[SeF_6]$ were prepared as previously reported [68]. The solvents dichloromethane and acetonitrile were dried by standard methods, and freshly distilled prior to use. NMR spectra were recorded in CD_2Cl_2 at 0 °C on a JEOL Eclipse 400 instrument, and chemical shifts are with respect to $CFCl_3$ (^{19}F, 376.1 MHz) and Me_2Se (^{77}Se, 76.3 MHz).

At USC, all reactions were carried out in Teflon-FEP ampules or stainless steel cylinders that were closed by stainless steel valves and had been passivated with ClF_3 prior to use. Volatile materials were handled in stainless steel/Teflon-FEP or grease-free Pyrex-glass vacuum lines [69]. Nonvolatile materials were handled in the dry argon atmosphere of a glove box. Raman spectra were recorded at −80 °C in the range 4000–80 cm^{-1} on a Bruker Equinox 55 FT-RA spectrophotometer using a Nd-YAG laser at 1064 nm with power levels less than 100 mW. Teflon-FEP tubes with stainless steel

Table 9
Calculated heats of formation in kcal/mol.

Molecule	ΔH_f (0 K)	ΔH_f (298 K)
SeF_4	−197.3	−202.9
SeF_5^-	−331.6	−338.2
$SeOF_2$	−126.7	−131.1
$SeOF_3^-$	−249.2	−254.7
SeO_2	−34.7	−38.1
SeO_2F^-	−161.2	−165.7

valves were used as sample containers. NMR spectra were recorded at 470.51 MHz (^{19}F) and 95.36 MHz (^{77}Se) on a Bruker AMX 500 spectrometer using neat compounds or solutions of the compounds in acetonitrile or DMSO in sealed 4 mm Teflon-FEP sample tubes. Neat $CFCl_3$ (0.00 ppm) and $(CH_3)_2Se$ (0.00 ppm) were used as external references for ^{19}F and ^{77}Se, respectively. The starting materials SeO_2, $[P(C_6H_5)_4]Cl$, $[((C_6H_5)_3P)_2N]Cl$ (all from Aldrich), and ClF_3 (Matheson Co.) were used without further purification. The HF (Matheson Co.) was dried by storage over BiF_5 (Ozark Mahoning) [70]. Solvents were dried by standard methods and freshly distilled prior to use. $[P(C_6H_5)_4][HF_2]$ and $[((C_6H_5)_3P)_2N][HF_2]$ were prepared from $[P(C_6H_5)_4]N_3$ and $[((C_6H_5)_3P)_2N]N_3$, respectively, and HF. $[P(C_6H_5)_4]N_3$ and $[((C_6H_5)_3P)_2N]N_3$ were prepared from $[P(C_6H_5)_4]Cl$ and $[((C_6H_5)_3P)_2N]Cl$, respectively, and NaN_3 by ion-exchange [71]. Literature methods were used for the preparation of anhydrous $[N(CH_3)_4]F$ [72], H_2SeO_3 [73], and $Cs[SeO_2F]$ [16].

3.2. Preparation and analytical data of the fluoroselenites

[PNP][SeF5]: Silver fluoride (1.77 mmol) was added at room temperature to a solution of SeF_4 (1.77 mmol) in CH_3CN (4 mL). The resulting solution was stirred for 2 h and then [PNP]Cl (1.77 mmol) was added. After additional stirring for 30 min, the pale yellow solution was decanted from a gray precipitate and all volatile material was pumped off, yielding a colorless solid

[PNP]2[SeF6]: Silver fluoride (3.55 mmol) was added at room temperature to a solution of SeF_4 (1.77 mmol) in CH_3CN (6 mL). The resulting solution was stirred for 2 h and then [PNP]Cl (3.55 mmol) was added. After additional stirring for 30 min, the pale yellow solution was decanted from a gray precipitate and all volatile material was pumped off, yielding a colorless solid. ^{19}F NMR δ 41.5 (br) ppm; ^{77}Se NMR δ 1253 ppm

[PNP][SeOF3]: This compound was obtained as a by-product in the preparation of [PNP][SeF_5]. The reaction of $SeOF_2$, which was present in our sample of SeF_4, with AgF in CH_2Cl_2 furnished [PNP][$SeOF_3$] as colorless crystals suitable for X-ray analysis

SeF_4: A sample of SeO_2 (100 mmol) was loaded into a 75 mL stainless steel cylinder. The cylinder was evacuated, cooled to −196 °C, and HF (180 mmol) and ClF_3 (140 mmol) were condensed in. The reaction mixture was allowed to warm to ambient temperature. After 12 h, all volatile material was pumped off through traps at −45 and −196 °C. The −45 °C trap contained 95 mmol of pale yellow SeF_4.

$SeOF_2$: A sample of SeO_2 (30 mmol) was loaded into a 15 mL stainless steel cylinder. The cylinder was connected to the steel line, evacuated and SeF_4 (25 mmol) condensed in at −196 °C. The reaction mixture was warmed to ambient temperature. After 10 h, the $SeOF_2$ was pumped off, collected in a trap at −196 °C, and 22 mmol of $SeOF_2$ was obtained as pale yellow liquid.

$A^+[SeF_5]^-$, $(A^+)_2[SeF_6]^{2-}$ and $A^+[SeOF_3]^-$ ($A = [N(CH_3)_4]$, $[P(C_6H_5)_4]$, $[((C_6H_5)_3P)_2N]$): Stoichiometric amounts of SeF_4 or $SeOF_2$, respectively, were condensed onto frozen solutions of $A^+[HF_2]^-$ (0.30 mmol) in 1.5 mL CH_3CN at −196 °C. The reaction mixtures were stirred at ambient temperature. After 30 min, all volatile material was pumped off from the pale orange solutions, leaving behind off-white solids. Single crystals of $[((C_6H_5)_3P)_2N][SeF_5]$ were grown from CH_3CN solution by slow evaporation of the solvent in vacuo.

3.3. X-ray crystallography

At LMU, an Oxford Xcalibur diffractometer with a CCD area detector was employed for the data collection using Mo Kα radiation. The structure was solved using direct methods (SIR97) [74] and refined by full-matrix least squares on F^2 (SHELXL) [75]. All non-hydrogen atoms were refined anisotropically. Satisfactory atomic positions of the solvent molecules in [PNP][$SeOF_3$] could not be determined reliably. Therefore, the disordered solvent molecules were treated as a diffuse contribution using the program SQUEEZE [76,77] SQUEEZE calculated 338.0 Å^3 of void space per unit cell and 86 electrons; 2 molecules of dichloromethane require 84 electrons per unit cell.

At USC, the single crystal X-ray diffraction data of [((C6H5)3P)2N][SeF5] were collected on a Bruker 3-circle platform diffractometer, equipped with a SMART CCD (APEX) detector with the χ-axis fixed at 54.74°, and using Mo Kα radiation (Graphite monochromator) from a fine-focus tube. The diffractometer was equipped with an LT-3 apparatus for low-temperature data collection using controlled liquid nitrogen boil off. Cell constants were determined from 60 ten-second frames. A complete hemisphere of data was scanned on omega (0.3°) with a run time of 10-s per frame at a detector resolution of 512 × 512 pixels using the SMART software package [78]. A total of 1271 frames were collected in three sets and a final set of 50 frames, identical to the first 50 frames, was also collected to determine any crystal decay. The frames were then processed on a PC, running Windows 2000 software, by using the SAINT software package [79] to give the *hkl* files corrected for Lp/decay. The absorption correction was performed using the SADABS program [80]. The structure was solved by the direct method using the SHELX-90 program and refined by the least squares method on F2, SHELXL-97 incorporated in SHELXTL Suite 6.12 for Windows NT/2000 [75]. All non-hydrogen atoms were refined anisotropically. For the anisotropic displacement parameters, the U_{eq} is defined as one third of the trace of the orthogonalized U_{ij} tensor. ORTEP drawings were prepared using the ORTEP-3 for Windows V1.076 program [81]. Further details of the crystal structure investigations reported in this paper may be obtained from the Cambridge Crystallographic Data Centre (CCDC), 12 Union Road, Cambridge CB2 1EZ (UK) (fax: +44 1223 336 033 or email: deposit@ccdc cam ac uk) by quoting the depository numbers CCDC 686702 and 641947.

3.4. Computational details

Geometries were initially optimized at the density functional theory level with the B3LYP exchange-correlation functional [35,36] and the standard aug-cc-pV*n*Z, with n = D and T, basis sets were used for O and F [33]. A small core relativistic effective core potential (RECP) was used for Se, which subsumes the ($1s^2$, $2s^2$, $2p^6$,) orbital space into the 10-electron core, and a 24 electron space ($3s^2$, $3p^6$, $4s^2$, $3d^{10}$ and $4p^4$) with the electrons handled explicitly [34]. We denote this combination of basis sets as aug-cc-pVnZ. Only the spherical component subset (e.g., 5-term d functions, 7-term f functions, etc.) of the Cartesian polarization functions were used. Frequencies including the IR and Raman intensities were calculated with the B3LYP functional as well as with the MPW1PW91 exchange-correlation functional. The B3LYP geometries were used for the starting point for optimizations at the CCSD(T) level with the aug-cc-pVnZ basis sets for n = D, T, and in some cases Q. Frequencies were calculated at the CCSD(T)/aug-cc-pVDZ level for some molecules. Only the 4s and 4p electrons on Se

and the 2s and 2p electrons in O and F were correlated in the valence electron correlation calculations. The ZORA NMR calculations [40–45] were done, as described above, with the ADF code [39] at the B3LYP/aVTZ-PP geometries. NMR calculations were also done with the B3LYP and BLYP [36,38] functionals with the aug-cc-pVDZ and Ahlrichs TZ2P [37] basis sets.

The heat of formation calculations were done at the CCSD(T) level. For the open shell atomic calculations, we used the R/UCCSD(T) (restricted method for the starting Hartree–Fock wavefunction and then relaxed the spin restriction in the coupled cluster portion of the calculation) approach [82]. The CCSD(T)/aug-cc-pVnZ valence energies were extrapolated to the complete basis set (CBS) limit by using a mixed exponential/Gaussian function of the form [83]:

$$E(n) = E_{\mathrm{CBS}} + \mathrm{Be}^{-(n-1)} + \mathrm{Ce}^{-(n-1)^2} \quad (1)$$

with $n = 2$ (aug-cc-pVDZ), 3 (aug-cc-pVTZ), 4 (aug-cc-pVQZ). Core-valence corrections, ΔE_{CV}, were obtained as the difference between frozen-core and all-electrons correlated calculations at the CCSD(T)/cc-pwCVTZ-PP level [84]. A scalar relativistic correction, ΔE_{SR}, due to the F and O atoms was evaluated from the expectation values for the two dominant terms in the Breit–Pauli Hamiltonian (the mass-velocity and one-electron Darwin (MVD) corrections) [85] from configuration interaction singles and doubles (CISD) calculations with a VTZ basis set at the CCSD(T)/aug-cc-pVTZ geometry. Any "double counting" of the relativistic effect on the Se when applying a MVD correction to an energy, which already includes most of the relativistic effects via the RECP, is small. A second relativistic correction is due to atomic spin orbit effects and the values are 0.22 kcal/mol for O, 0.39 for F and 2.70 kcal/mol for Se were taken from the excitation energies compiled by Moore [86]. By combining our computed ΣD_0 values given by the following expression:

$$\sum D_0 = \Delta E_{\mathrm{elec}}(\mathrm{CBS}) - \Delta E_{\mathrm{ZPE}} + \Delta E_{\mathrm{CV}} + \Delta E_{\mathrm{SR}} + \Delta E_{\mathrm{SO}} \quad (2)$$

with the known [87,88] heats of formation at 0 K for the elements, $\Delta H_{\mathrm{f}}^{0}(\mathrm{O}) = 58.99$ kcal/mol, $\Delta H_{\mathrm{f}}^{0}(\mathrm{F}) = 18.47 \pm 0.07$ kcal/mol, and $\Delta H_{\mathrm{f}}^{0}(\mathrm{Se}) = 54.11$ kcal/mol, we can derive $\Delta H_{\mathrm{f}}^{0}$ values for the molecules under study. Heats of formation at 298 K were obtained by following the procedures outlined by Curtiss et al. [89].

All CCSD(T) calculations were performed with the MOLPRO program system [90] on the Dell Intel cluster at UA or on a Penguin AMD cluster at UA. The DFT and nonrelativistic NMR chemical shift calculations were done with the Gaussian program system [91] The ZORA NMR calculations were done with the ADF program system [39].

Acknowledgements

Financial support from the University of Munich, the Fonds der Chemischen Industrie, and the Deutsche Forschungsgemeinschaft (KL636/10-1) is gratefully acknowledged. The work at USC was financially supported by the National Science Foundation, the Air Force Office of Scientific Research, the Office of Naval Research, and the Defense Threat Reduction Agency. This research was supported, in part, by the U.S. Department of Energy, Office of Basis Energy Research, Chemical Sciences, in the geosciences program.

References

[1] W. Nakanishi, S. Hayashi, J. Phys. Chem. A 103 (1999) 6074–6081.
[2] R. Kniep, L. Korte, R. Kryschi, W. Poll, Angew. Chem., Int. Ed. 23 (1984) 388–389.
[3] K. Seppelt, Z. Anorg. Allg. Chem. 416 (1975) 12–18.
[4] I.C. Bowater, R.D. Brown, F.R. Burden, J. Mol. Spectrosc. 28 (1968) 454–460.
[5] R. Damerius, P. Huppmann, D. Lentz, K. Seppelt, J. Chem. Soc., Dalton Trans. (1984) 2821–2826.
[6] A.R. Mahjoub, D. Leopold, K. Seppelt, Z. Anorg. Allg. Chem. 618 (1992) 83–88.
[7] K.O. Christe, E.C. Curtis, C.J. Schack, D. Pilipovich, Inorg. Chem. 11 (1972) 1679–1682.
[8] A.R. Mahjoub, X. Zhang, K. Seppelt, Chem. Eur. J. 1 (1995) 261–265.
[9] K.H. Moock, R.T. Boere, J. Fluorine Chem. 68 (1994) 175–179.
[10] I.C. Bowater, R.D. Brown, F.R. Burden, J. Mol. Spectrosc. 23 (1967) 272–279.
[11] R. Paetzold, K. Aurich, Z. Anorg. Allg. Chem. 315 (1962) 72–78.
[12] J.A. Rolfe, L.A. Woodward, Trans. Faraday Soc. 51 (1955) 778–780.
[13] E.B.R. Prideaux, C.B. Cox, J. Chem. Soc. (1928) 739–745.
[14] E.B.R. Prideaux, C.B. Cox, J. Chem. Soc. (1927) 928–929.
[15] C. Feldmann, M. Jansen, Chem. Ber. 127 (1994) 2173–2176.
[16] J. Milne, Inorg. Chem. 17 (1978) 3592–3595.
[17] E.J. Baran, J. Fluorine Chem. 10 (1977) 255–259.
[18] R.J. Gillespie, P. Spekkens, J.B. Milne, D. Moffett, J. Fluorine Chem. 7 (1976) 43–54.
[19] R. Paetzold, K. Aurich, Z. Anorg. Allg. Chem. 335 (1965) 281–288.
[20] J. Milne, P. Lahaie, Inorg. Chem. 22 (1983) 2425–2428.
[21] R. Paetzold, K. Aurich, Z. Anorg. Allg. Chem. 348 (1966) 94–106.
[22] R. Paetzold, K. Aurich, Z. Chem. 6 (1966) 152–153.
[23] A. Kornath, D. Kadzimirsz, R. Ludwig, Inorg. Chem. 38 (1999) 3066–3069.
[24] U. Kessler, M. Jansen, Z. Anorg. Allg. Chem. 627 (2001) 1782–1786.
[25] T.M. Klapötke, B. Krumm, P. Mayer, I. Schwab, Acta Crystallogr. E 61 (2005) o2984–o2986.
[26] L. Wang, Int. J. Mass Spectrom. 264 (2007) 84–91.
[27] M. Atanasov, D. Reinen, Inorg. Chem. 43 (2004) 1998–2012.
[28] Q. Li, W. Xu, Y. Xie, H.F. Schaefer III, J. Phys. Chem. A 103 (1999) 7496–7505.
[29] M. Alexandre, P. Rigny, Can. J. Chem. 52 (1974) 3676–3681.
[30] K. Wolinski, J.F. Hinton, P. Pulay, J. Am. Chem. Soc. 112 (1990) 8251–8260.
[31] C. Adamo, V. Barone, J. Chem. Phys. 108 (1998) 664–675.
[32] J.P. Perdew, Y. Wang, Phys. Rev. B 45 (1991) 13244.
[33] (a) T.H. Dunning Jr., J. Chem. Phys. 90 (1989) 1007–1023;
(b) R.A. Kendall, T.H. Dunning Jr., R.J. Harrison, J. Chem. Phys. 96 (1992) 6796–6806;
(c) D.E. Woon, T.H. Dunning Jr., J. Chem. Phys. 98 (1993) 1358–1371;
(d) T.H. Dunning Jr., K.A. Peterson, A.K. Wilson, J. Chem. Phys. 114 (2001) 9244–9253;
(e) A.K. Wilson, D.E. Woon, K.A. Peterson, T.H. Dunning Jr., J. Chem. Phys 110 (1999) 7667–7676.
[34] (a) K.A. Peterson, J. Chem. Phys. 119 (2003) 11099–11112;
(b) K.A. Peterson, D. Figgen, E. Goll, H. Stoll, M. Dolg, J. Chem. Phys. 119 (2003) 11113–11123.
[35] A.D. Becke, J. Chem. Phys. 98 (1993) 5648–5652.
[36] C. Lee, C.W. Yang, R.G. Parr, Phys. Rev. B 37 (1988) 785–789.
[37] A. Schäfer, H. Horn, R. Ahlrichs, J. Chem. Phys. 97 (1992) 2571–2577.
[38] A.D. Becke, Phys. Rev. A 38 (1988) 3098–3100.
[39] (a) ADF 2004.01, ADF Users Guide, SCM, Theoretical Chemistry, Vrije Universiteit, Amsterdam, http://www.scm.com.
(b) G. te Velde, F.M. Bickelhaupt, E.J. Baerends, C. Fonseca Guerra, J.A. van Gisbergen, J.G. Snijders, T. Ziegler, J. Comput. Chem. 22 (2001) 931–967.
[40] G. Schreckenbach, T. Ziegler, J. Phys. Chem. 99 (1995) 606–611.
[41] G. Schreckenbach, T. Ziegler, Int. J. Quantum Chem. 61 (1997) 899–918.
[42] S.K. Wolff, T. Ziegler, J. Chem. Phys. 109 (1998) 895–905.
[43] S.K. Wolff, T. Ziegler, E. van Lenthe, E.J. Baerends, J. Chem. Phys. 110 (1999) 7689–7698.
[44] E. van Lenthe, E.J. Baerends, J.G. Snijders, J. Chem. Phys. 99 (1993) 4597–4610.
[45] J. Autschbach, T. Ziegler, in: M. Kaupp, M. Buhl, V.G. Malkin (Eds.), Calculation of NMR and EPR Parameters: Theory and Application, Wiley-VCH & Co., Weinheim, 2004, pp. 249–264.
[46] H. Poleschner, K. Seppelt, Chem. Eur. J. 10 (2004) 6565–6574.
[47] T. Maaninen, H.M. Tuononen, K. Kosunen, R. Oilunkaniemi, J. Hitola, R. Laitinen, T. Chivers, Z. Anorg. Allg. Chem. 630 (2004) 1947–1954.
[48] G. Schreckenbach, Y. Ruiz-Morales, T. Ziegler, J. Chem. Phys. 104 (1996) 8605–8612.
[49] J. Pilme, E.A. Robinson, R.J. Gillespie, Inorg. Chem. 45 (2006) 6198–6204.
[50] D.A. Dixon, W.A. de Jong, K.A. Peterson, K.O. Christe, G.J. Schrobilgen, J. Am. Chem. Soc. 127 (2005) 8627–8634.
[51] D.A. Dixon, D.J. Grant, K.O. Christe, K.A. Peterson, Inorg. Chem. 47 (2008) 5485–5494.
[52] D.A. Dixon, T.-H. Wang, D.J. Grant, K.A. Peterson, K.O. Christe, Inorg. Chem. 46 (2007) 10016–10021.
[53] M. Kaupp, Ch. van Wuellen, R. Franke, F. Schmitz, W. Kutzelnigg, J. Am. Chem. Soc. 118 (1996) 11939–11950.
[54] M. Klobukowski, J. Comput. Chem. 14 (1993) 1234–1239.
[55] A. Ellern, J.A. Boatz, K.O. Christe, T. Drews, K. Seppelt, Z. Anorg. Allg. Chem. 628 (2002) 1991–1999.
[56] H. Oberhammer, K.O. Christe, Inorg. Chem. 21 (1982) 273–275.
[57] G.C. Pimentel, J. Chem. Phys. 19 (1951) 446–448.
[58] R.J. Hach, R.E. Rundle, J. Am. Chem. Soc. 73 (1951) 4321–4324.
[59] I. Love, J. Phys. Chem. A 113 (2009) 2640–2646.
[60] R.F.W. Bader, Atoms in Molecules—A Quantum Theory, Oxford University Press, Oxford, 1990.
[61] K.O. Christe, H. Oberhammer, Inorg. Chem. 20 (1981) 296–297.
[62] K.O. Christe, XXIVth International Congress of Pure and Applied Chemistry, vol. 4, 1974, 115–141.
[63] K.O. Christe, W. Sawodny, P. Pulay, J. Mol. Struct. 21 (1974) 158–164.
[64] R.S. Berry, J. Chem. Phys. 32 (1960) 933–938.

[65] (a) D. Feller, D.A. Dixon, J. Phys. Chem. A 104 (2000) 3048–3056;
(b) D. Feller, D.A. Dixon, J. Chem. Phys. 115 (2001) 3484–3496;
(c) D.A. Dixon, D. Feller, K.A. Peterson, J. Chem. Phys. 115 (2001) 2576–2581;
(d) D. Feller, D.A. Dixon, J. Phys. Chem. A 107 (2003) 9641–9651;
(e) D.A. Dixon, D. Feller, K.O. Christe, W.W. Wilson, A. Vij, V. Vij, H.D.B. Jenkins, R.M. Olson, M.S. Gordon, J. Am. Chem. Soc. 126 (2004) 834–843;
(f) D.A. Dixon, M. Gutowski, J. Phys. Chem. A 109 (2005) 5129–5135;
(g) L. Pollack, T.L. Windus, W.A. de Jong, D.A. Dixon, J. Phys. Chem. A 109 (2005) 6934–6938;
(h) D. Feller, K.A. Peterson, D.A. Dixon, J. Chem. Phys. 129 (2008) 204105 (32 pp.);
(i) B. Ruscic, A.F. Wagner, L.B. Harding, R.L. Asher, D. Feller, D.A. Dixon, K.A. Peterson, Y. Song, X. Qian, C. Ng, J. Liu, W. Chen, D.W. Schwenke, J. Phys. Chem. A 106 (2002) 2727–2747.
[66] K.O. Christe, D.A. Dixon, D. McLemore, W.W. Wilson, J. Sheehy, J.A. Boatz, J. Fluorine Chem. 101 (2000) 151–153; Chem. Eng. News, pp. 48–49, March 3, 2003.
[67] D.F. Shriver, M.A. Drezdzon, The Manipulation of Air Sensitive Compounds, Wiley, New York, 1986.
[68] T.M. Klapötke, B. Krumm, M. Scherr, R. Haiges, K.O. Christe, Angew. Chem., Int. Ed. 46 (2007) 4686–8690.
[69] K.O. Christe, W.W. Wilson, C.J. Schack, R.D. Wilson, Inorg. Synth. 24 (1986) 39–48.
[70] K.O. Christe, W.W. Wilson, C.J. Schack, J. Fluorine Chem. 11 (1978) 71–85.
[71] R. Haiges, T. Schroer, M. Yousufuddin, K.O. Christe, Z. Anorg. Allg. Chem. 631 (2005) 2691–2695.
[72] K.O. Christe, W.W. Wilson, R.D. Wilson, R. Bau, J. Feng, J. Am. Chem. Soc. 112 (1990) 7619–7625.
[73] A. Rosenheim, L. Krause, Z. Anorg. Allg. Chem. 118 (1921) 177–192.
[74] A. Altomare, G. Cascarano, C. Giacovazzo, A. Guagliardi, A.G.G. Moliterni, M.C. Burla, G. Polidori, M. Camalli, R. Spagna, SIR97: A New Program for Solving and Refining Crystal Structures, Istituto de Cristallografia, Bari, Italy, 1997 http://www.ic.cnr.it/sir97.php.
[75] (a) G.M. Sheldrick, SHELXS-90, Program for the Solution of Crystal Structure, University of Göttingen, Germany, 1990, SHELXL-97, Program for the Refinement of Crystal Structure, University of Göttingen, Germany, 1997.;
(b) SHELXTL 6.12 for Windows NT/2000, Program library for Structure Solution and Molecular Graphics, Bruker AXS, Madison, WI, 2000.
[76] A.L. Spek, Squeeze software, University of Utrecht, The Netherlands, 2001.
[77] P. Van der Sluis, A.L. Spek, Acta Crystallogr. A 46 (1990) 194–201.
[78] SMART V 5.625, Software for the CCD Detector System, Bruker AXS Madison, WI, 2001.
[79] SAINT V 6.22, Software for the CCD Detector System, Bruker AXS Madison, WI, 2001.
[80] SADABS, Software for the CCD Detector System, Bruker AXS Madison, WI, 2001.
[81] L.J. Farrugia, J. Appl. Cryst. 30 (1997) 565.
[82] (a) P.J. Knowles, C. Hampel, H.-J. Werner, J. Chem. Phys. 99 (1993) 5219–5227;
(b) M.J.O. Deegan, P.J. Knowles, J. Chem. Phys. Lett. 227 (1994) 321–326.
[83] K.A. Peterson, D.E. Woon, T.H. Dunning Jr., J. Chem. Phys. 100 (1994) 7410–7415.
[84] (a) K.A. Peterson, T.H. Dunning Jr., J. Chem. Phys. 117 (2002) 10548–10560;
(b) D.E. Woon, T.H. Dunning Jr., J. Chem. Phys. 98 (1993) 1358–1371.
[85] E.R. Davidson, Y. Ishikawa, G.L. Malli, Chem. Phys. Lett. 84 (1981) 226–227.
[86] C.E. Moore, Atomic energy levels as derived from the analysis of optical spectra, Vol. 1, H to V, U.S. National Bureau of Standards Circular 467, U.S. Department of Commerce, National Technical Information Service, COM-72-50282, Washington, DC, 1949.
[87] M.W. Chase, Jr., NIST-JANAF Tables (4th edition), J. Phys. Chem. Ref. Data, Mono. 9, Suppl. 1 (1998).
[88] D.D. Wagman, W.H. Evans, V.B. Parker, R.H. Schumm, I. Halow, S.M. Bailey, K.L. Churney, R.L. Nuttall, J. Phys. Chem. Ref. Data 11 (1982) (Suppl. 2).
[89] L.A. Curtiss, K. Raghavachari, P.C. Redfern, J.A. Pople, J. Chem. Phys. 106 (1997) 1063–1079.
[90] H.-J. Werner, P.J. Knowles, R. Lindh, F.R. Manby, M. Schütz, P. Celani, T. Korona, A. Mitrushenkov, G. Rauhut, T.B. Adler, R.D. Amos, A. Bernhardsson, A. Berning, D.L. Cooper, M.J.O. Deegan, A.J. Dobbyn, F. Eckert, E. Goll, C. Hampel, G. Hetzer, T. Hrenar, G. Knizia, C. Köppl, Y. Liu, A.W. Lloyd, R.A. Mata, A.J. May, S.J. McNicholas, W. Meyer, M.E. Mura, A. Nicklaß, P. Palmieri, K. Pflüger, R. Pitzer, M. Reiher, U. Schumann, H. Stoll, A.J. Stone, R. Tarroni, T. Thorsteinsson, M. Wang, A. Wolf, MOLPRO, Version 2009. A Package of ab initio Programs, University of Cardiff/Universität Stuttgart, Wales, UK/Stuttgart, Germany, 2009.
[91] M.J. Frisch, G.W. Trucks, H.B. Schlegel, G.E. Scuseria, M.A. Robb, J.R. Cheeseman, J.A. Montgomery Jr., T. Vreven, K.N. Kudin, J.C. Burant, J.M. Millam, S.S. Iyengar, J. Tomasi, V. Barone, B. Mennucci, M. Cossi, G. Scalmani, N. Rega, G.A. Petersson, H. Nakatsuji, M. Hada, M. Ehara, K. Toyota, R. Fukuda, J. Hasegawa, M. Ishida, T. Nakajima, Y. Honda, O. Kitao, H. Nakai, M. Klene, X. Li, J.E. Knox, H.P. Hratchian, J.B. Cross, V. Bakken, C. Adamo, J. Jaramillo, R. Gomperts, R.E. Stratmann, O. Yazyev, A.J. Austin, R. Cammi, C. Pomelli, J.W. Ochterski, P.Y. Ayala, K. Morokuma, G.A. Voth, P. Salvador, J.J. Dannenberg, V.G. Zakrzewski, S. Dapprich, A.D. Daniels, M.C. Strain, O. Farkas, D.K. Malick, A.D. Rabuck, K. Raghavachari, J.B. Foresman, J.V. Ortiz, Q. Cui, A.G. Baboul, S. Clifford, J. Cioslowski, B.B. Stefanov, G. Liu, A. Liashenko, P. Piskorz, I. Komaromi, R.L. Martin, D.J. Fox, T. Keith, M.A. Al-Laham, C.Y. Peng, A. Nanayakkara, M. Challacombe, P.M.W. Gill, B. Johnson, W. Chen, M.W. Wong, C. Gonzalez, J.A. Pople, Gaussian 03. Revision E.01, Gaussian, Inc., Wallingford, CT, 2004.